J Therm Anal Calorim (2009) 98:639–644
DOI 10.1007/s10973-009-0508-3

Rheological techniques for the determination of the crystallization kinetics of a polypropylene–EPR copolymer

Stefano Acierno · Rossana Pasquino · Nino Grizzuti

Rheological Analysis of Polymers/Special Chapter

Abstract In this article, we show that the crystallization behaviour of a rubber-filled polypropylene, under isothermal conditions, can be monitored by means of parallel plate rheometry and differential scanning calorimetry. Data collected with different instruments can be compared only after performance of accurate temperature calibration. The complex modulus as obtained from dynamic mechanical measurements can be related to the crystalline content by use of appropriate mathematical relationships. An empirical power law model is used to correlate the crystalline content to the rheological function. Excellent agreement between rheological and calorimetric data is found. Furthermore, it is shown that rheology can be used to achieve additional information on the structural evolution of the crystallizing system.

Keywords Polymer crystallization · Crystallization kinetics · Rheological measurements · iPP–EPR copolymer

Introduction

During the last decades, the use of rheological techniques to study polymer crystallization has gained increasing consensus. When a polymeric liquid is cooled below its melting temperature, crystalline structures start to develop. As the material gradually transforms into a semicrystalline solid, the viscoelastic properties of the system (such as viscoelastic moduli) change by orders of magnitude. For this reason, rheometry provides a very sensitive tool to study crystallization phenomena. Rheological functions can be used to calculate the evolution of relative crystallinity, $x(t)$, once a functional relation is assumed. Khanna [1], for example, proposed a linear relation between elastic modulus and crystallinity and used this approach to study the crystallization kinetics of different, nucleated and unnucleated, polymers.

The main advantage of rheological techniques, over traditional ones such as DSC, is that they can be more sensitive when crystallization kinetics are slow [2] and can provide information on the morphology of the crystallizing material [3]. On the other hand, the major drawback in the use of rheological techniques is that a universal correlation between viscoelastic properties and crystallinity is still missing. Moreover, for meaningful comparison of rheological and DSC data collected during crystallization, an accurate temperature calibration of the two instruments is a fundamental requisite. To overcome these limitations, Kiewit et al. [4] have recently combined a rheometer and a DSC into a single instrument to compare the evolution of rheological properties to crystallinity as measured from heat flow integration. While this RheoDSC instrument was shown to provide reliable measurements, a systematic study on crystallizing systems is still missing.

Aim of this study is to correlate the rheological and thermal response during crystallization and to study the possibility to interpret the rheological results in terms of crystallinity evolution.

S. Acierno (✉)
Dipartimento di Ingegneria, Università degli Studi del Sannio, Piazza Roma 21, 82100 Benevento, Italy
e-mail: stefano.acierno@unisannio.it

R. Pasquino · N. Grizzuti
Dipartimento di Ingegneria Chimica, Università degli Studi di Napoli Federico II, Piazzale Tecchio 80, 80125 Naples, Italy

Experimental

Materials

A semicrystalline polymer (HIFAX BA 238 G3, by Montell, Ferrara, Italy) was selected as the testing material. It is a heterophasic polypropylene with an excellent stiffness/impact strength balance. Impact strength is improved by an ethylene-propylene rubber phase (EPR, copolymer C2–C3 at about 50% of each component) dispersed in the polypropylene matrix. The rubber weight percentage is about 26, a small percentage of talc (about 1.5%) is also present in the resin.

Methods

Thermal behaviour and overall crystallization kinetics were analysed with a differential scanning calorimeter (Shimadtzu DSC60), equipped with an intra-cooler to permit operations of down to about −60 °C. Temperature and heat flux were calibrated as described in the next section using high-purity indium.

Crystallization experiments in the DSC instrument were conducted according to the following standard procedure. Polymeric samples (with a mass of about 6 mg) were melted for 10 min at 210 °C, under dry nitrogen atmosphere, to eliminate prior thermal history. Samples were then cooled at a rate of 20 °C min^{-1} to the crystallization temperature T_c and maintained under isothermal conditions for a time long enough to complete crystallization. During crystallization the heat flux, $\dot{q}$, was recorded as a function of time, t, and was used to calculate the relative degree of crystallization, $x(t)$, according to the following relation:

$$x(t) = \frac{\int_0^t \dot{q}(t)\mathrm{d}t}{\int_0^\infty \dot{q}(t)\mathrm{d}t} \quad (1)$$

Rheological measurements were performed using two different instruments: (i) a stress-controlled rheometer, SR200 from Rheometric Scientific Inc., equipped with parallel plates (plate diameter $D_1 = 25$ mm) and heated plates temperature control option; and (ii) a strain-controlled instrument (ARES LS with 2 K FRT force transducer from TA Instruments) equipped with parallel plates ($D_2 = 7.9$ mm) and a forced air convection oven. Temperature sensors of the two instruments were calibrated as described in the next section using high-purity indium.

Rheological experiments during crystallization were performed according to the following procedure. The rheometer plates were heated at 210 °C; the as-received polymer pellets were placed on the bottom plate, melted and pressed to form homogeneous discs with a diameter $D_1 = 25$ mm and a thickness $h_1 = 1$ mm (or, alternatively $D_2 = 7.9$ mm and $h_2 = 0.5$ mm). After a thermal annealing of 10 min at 210 °C, samples were cooled at a rate of 20 °C min^{-1} to the crystallization temperature T_c and maintained under isothermal conditions. (In all cases the cooling time was much shorter than the crystallization time). During isothermal crystallization a small amplitude oscillatory shear flow, with a frequency of 1 rad s^{-1}, was applied to the sample and the evolution of complex modulus, G^*, was recorded as a function of time. On the SR200 rheometer, the amplitude of stress oscillation was initially set at 100 Pa and was gradually increased with time to keep the angular displacement within instrumental limits. On the ARES rheometer, the amplitude of strain oscillation was initially set at 1% and was gradually reduced with time to keep the torque within transducer sensitivity. In all, cases prior to the experimental campaign, it was verified that oscillations were sufficiently small so as not to influence crystallization phenomena within the sample. Moreover, it should be noted that dimensional changes of the sample occur during crystallization due to the different densities between liquid and crystalline phases. Dimensional changes have two main effects: on the one hand, the sample would be subjected to a tensile stress caused by a thickness reduction; on the other hand, the effective diameter of the sample would be smaller than the initial one thus causing erroneous calculation of the viscoelastic properties. This latter error can be as large as 10% as the complex modulus is related to D^{-4}.

In order to minimize errors due to dimensional variations the gap between parallel plates was varied during the experiments in such a way to keep a null compressive force on the samples.

Temperature calibration

Temperature calibration of the two rheometers and the DSC instrument was performed using a high purity (99.999%) indium standard with a melting temperature of 156.6 °C.

The temperature sensor of the DSC was calibrated observing the melting of a 3.8 mg indium sample during heating ramps from 140 to 180 °C at different heating rates. As indium approaches the melting temperature, the heat flux departs from its base line showing an endothermic (positive) peak (see Fig. 1). This melting peak is characterized by the temperature at which the heat flux starts to depart from its base line (*onset temperature*), by the temperature at which the heat flux reaches its maximum (*peak temperature*) and by the temperature at which the heat flux re-approaches the base line (*end temperature*). The onset temperature, which is often associated to the melting temperature of the material, can strongly depend on the

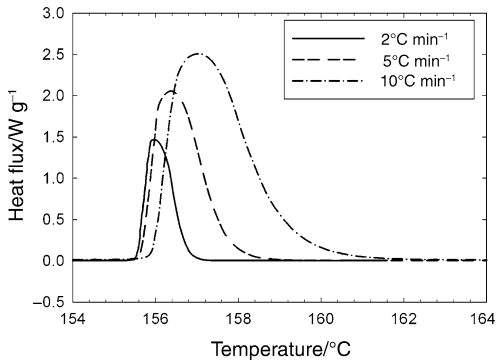

Fig. 1 DSC thermograms during scans at different heating rates. Endothermic peaks correspond to melting of a pure indium sample

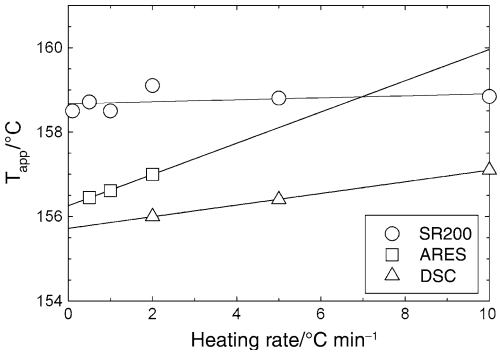

Fig. 2 Apparent (or measured) melting temperature of indium samples as a function of the heating rate as obtained for the SR200, ARES and DSC instruments

base line, which is arbitrarily drawn. On the contrary, the peak temperature can usually be detected with greater reproducibility. For this reason, it was decided to indicate the peak temperature as the apparent (or measured) melting temperature of the sample, T_{app}. As expected, T_{app} shows a shift towards higher values as the heating rate is increased.

Melting temperature versus heating rate data (see Fig. 2) show an increasing apparent melting temperature as a function of the heating rate; the intercept of the linear regression is the melting temperature of indium under isothermal condition. The experimental results can be compared to the melting temperature of indium (i.e. 156.6 °C) and used to obtain an isothermal temperature correction defined as $\Delta T_{DSC} = T_{true} - T_{app} = -0.9$ °C.

The rheometers were used with a parallel plates configuration and the temperature was monitored through the instrument thermocouple, placed below the bottom plate in contact with its metallic surface. A small piece of indium was placed between the two plates in central position. Notice that, as the piece of indium does not cover the entire plate area, the following data will be expressed in terms of torque and angular displacement instead of the more common rheological functions such as shear stress and shear strain.

In the SR200, a thin ($\sim$0.35 mm) piece of indium was placed between the 25-mm parallel plates, the oscillatory frequency was set to 1 rad s^{-1} and the torque amplitude to 3.67×10^{-4} Nm, while the temperature was varied from 120 to 180 °C with heating rates in the range from 0.5 to 10 °C min^{-1}. The evolution of angular displacement, θ, was monitored as a function of time. A sudden drop in the amplitude of angular displacement amplitude is observed in correspondence of the melting of indium. The temperature corresponding to the maximum in the time derivative of θ, $d\theta/dt$, is recorded as the apparent (or measured) melting temperature of the sample, T_{app}.

The above procedure is repeated at different heating rates thus obtaining the data also reported in Fig. 2, where linear regression of data is also plotted. The results show a poor dependency of T_{app} upon heating rate due to the design of the heating system. The intercept of the linear regression is the melting temperature of indium under isothermal conditions and allows for calculation of the isothermal temperature correction $\Delta T_{SR200} = T_{true} - T_{app} = -2.0$ °C.

In the ARES rheometer, a thin ($\sim$0.7 mm) piece of indium was placed between the 7.9-mm parallel plates, the oscillatory frequency was set at 10 rad s^{-1} and the amplitude of the angular displacement was set to 11 µrad. During experiments, the temperature was changed from 140 to 160 °C with heating rates ranging from 0.5 to 2 °C min^{-1}.

In this case, the evolution of the torque is monitored as a function of time. As the temperature within the sample reaches the melting temperature of indium a sudden decrease in the torque is observed. The temperature corresponding to the minimum in the time derivative of the torque is recorded as the apparent melting temperature of the sample. A typical experimental result, at a heating rate of 1 °C min^{-1}, is shown in Fig. 3 where an apparent melting temperature of 156.3 °C is observed.

Data of apparent melting temperature versus heating rate collected with the ARES rheometer, also reported in Fig. 2, show that the apparent melting temperature is very close to the actual melting temperature of pure indium, thus demonstrating a good accuracy of the thermal control. Following the procedure described above, the isothermal temperature correction $\Delta T_{ARES} = T_{true} - T_{app} = +0.3$ °C is obtained.

At the end of this calibration procedure, it was possible to perform isothermal experiments with great accuracy and, as a consequence, to compare data collected with the three different instruments.

As a demonstration of the accuracy of this calibration procedure, results collected during isothermal crystallization performed (according to the aforementioned procedure) at $T_c = 145$ °C with the three instruments are compared.

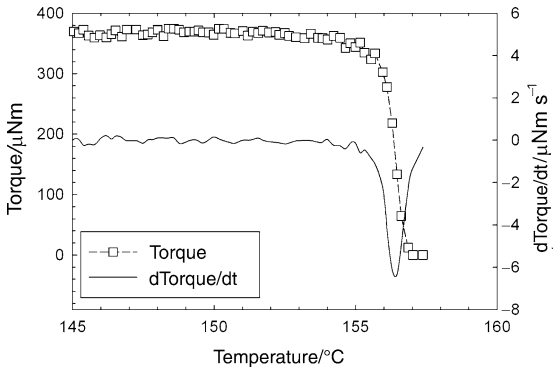

Fig. 3 Torque and torque derivative as a function of temperature during a heating scan at 1 °C min^{-1}. The sudden decrease in torque and downward peak in torque derivative correspond to melting of a pure indium sample

Data reported in Fig. 4 show that the complex modulus increases with time as a consequence of the crystallinity development. In particular, the complex modulus remains constant around a value of 7,000 Pa during the first 600 s (corresponding to an undercooled melt condition). After this time lag, G^* shows a gradual increase of several orders of magnitude and eventually reaches a final value of about 10 MPa (typical of semicrystalline polymers) at the end of the solidification process. The agreement between the G^* versus time curves collected with the two different rheometers is remarkable and shows that a very similar crystallization behaviour is obtained. It should be stressed that the disagreement in the final part of the curves is only apparent as data collected with the SR200 are unreliable due to the excessive stiffness of the sample. For this reason in the following only rheological data collected with the ARES rheometer will be presented.

In Fig. 4, the time evolution of the relative crystallinity as obtained from integration of the DSC signal is also reported. Comparison of rheological and calorimetric data shows that as crystallinity increases the complex modulus of the system increases as well; the structure development (as measured from the logarithmic modulus increase) and the crystallinity evolution proceed on the same time scale. When the complex modulus starts to deviate from its initial value, a 20% relative crystallinity has already developed.

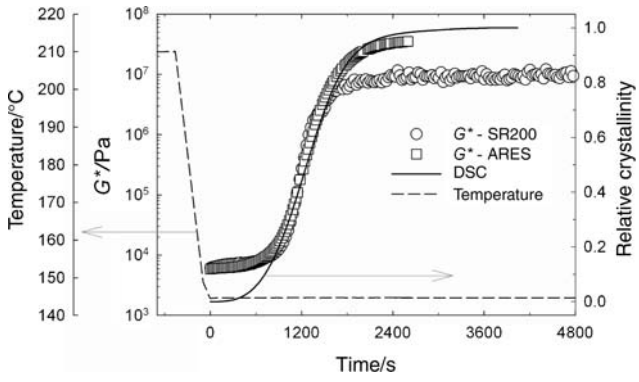

Fig. 4 Evolution of complex modulus (from SR200 and ARES rheometers) and relative crystallinity (from DSC) as a function of time during isothermal crystallization of iPP at 145.0 °C. For the sake of clarity the temperature profile is also drawn on the outer *y*-axis

Results and discussion

Calorimetric data collected under isothermal crystallization are reported in Fig. 5 in terms of heat flux versus time. Data show negative (exothermic) peaks that progressively flatten out as the crystallization temperature increases. The overall heat released during crystallization does not change significantly with crystallization temperature and shows an average value of 71 J g^{-1} (which corresponds to a 42% crystallinity of the iPP phase). Successive integration and normalization of thermograms allow to calculate the evolution of the relative crystallinity as a function of time, $x(t)$, as reported in Fig. 6.

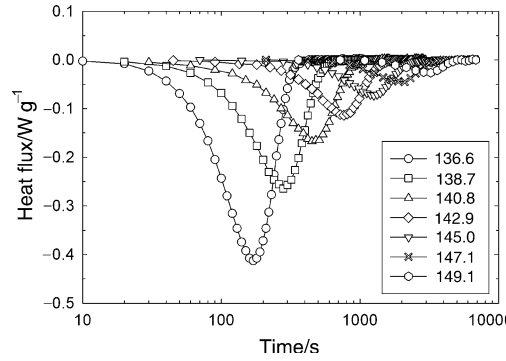

Fig. 5 Specific heat flux versus time during isothermal crystallization at different temperatures

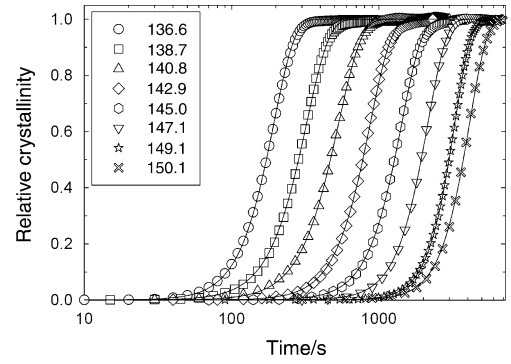

Fig. 6 Time evolution of relative crystallinity at different temperatures as calculated from integration and normalization of DSC thermograms (see Eq. 1). Lines through data points are regressions with Avrami equation (Eq. 2)

Isothermal crystallization kinetics were analysed using Avrami equation [5] expressed as follows [6]:

$$x(t) = 1 - \exp\left[-\ln(2) \cdot \left(\frac{t}{t_{0.5}}\right)^n\right] \quad (2)$$

where $t_{0.5}$ is the half-crystallization time and n is the Avrami exponent, which can be related to the mechanism of nucleation and to the form of crystal growth.

According to Eq. 2, the Avrami exponent can be obtained as the slope of a linear regression when $\log\{-\ln[1 - x(t)]\}$ is plotted versus $\log(t)$. $t_{0.5}$ is obtained as the time needed to reach a relative crystallinity of 50% and is independent of the value of n.

Figure 6 shows a good agreement between experimental data and predictions from Avrami equation (reported as continuous lines) in a wide crystallinity range.

Avrami exponent, as calculated from DSC data, is plotted as a function of reciprocal temperature in Fig. 7. Avrami exponent does not show a relevant dependence upon the crystallization temperature, with an average value $n = 3.2$ consistent with a three-dimensional crystal growth of predetermined nuclei. On the other hand, the half-crystallization time, also reported in Fig. 7, is found to be an increasing function of the crystallization temperature—as expected for crystallization of polymers under moderate undercoolings—and can be described by the following Arrhenius-like relation:

$$t_{0.5}(T_c) = \exp\left(A - \frac{E_a}{RT_c}\right) \quad (3)$$

where $A = 101.2$ is a dimensionless parameter, $E_a = 277.4$ kJ mol^{-1} K^{-1} is the activation energy, and R is the gas constant. It should be mentioned that this value for the activation energy is in line with data for polypropylene in the same temperature range while the half-crystallization time is one order of magnitude smaller than values reported for unnucleated iPPs [7].

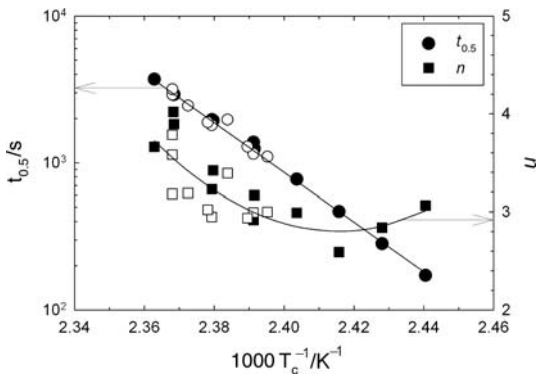

Fig. 7 Half-crystallization time and Avrami exponent as a function of reciprocal crystallization temperature. DSC data are plotted as *filled symbols*, while rheological data (treated using Eq. 6) are plotted as *empty symbols*. The line through the half-crystallization time data is Eq. 3, whereas the line through the Avrami exponent data is to guide the eye

Polymer crystallization can also be monitored using rheological measurements. In particular, isotherms in the temperature range between 144.3 and 149.1 °C were performed according to the protocol described in the "Experimental" section. Results at selected T_c's are shown in Fig. 8. The complex modulus G^* gradually increases as the system changes from an undercooled melt to a semi-crystalline solid. The initial complex modulus, G_0^*, and the final plateau value, G_∞^*, both decrease upon increasing temperature as expected for polymeric systems well above the glass-transition temperature. Differences in G_∞^* at the different temperatures are well visible thus showing a great sensitivity of the rheometer in detecting small variations (few °C) in the crystallization temperature. Furthermore, Fig. 8 shows slower crystallization dynamics as the temperature is increased as expected and already observed from DSC measurements.

As suggested by the data shown in Fig. 4, the viscoelastic modulus increases by orders of magnitude as crystallinity develops. Changes in the dynamic mechanical properties can be related to changes in the relative amounts of crystalline and amorphous phases.

On the one hand, amorphous and crystalline phases can be assumed to behave as two viscoelastic elements connected in parallel and subjected to the same deformation thus leading to the following relation:

$$x(t) = \frac{G^*(t) - G_0^*}{G_\infty^* - G_0^*} \quad (4)$$

Equation 4 is a "mixing rule" that has been often used to study crystallization kinetics of different materials [1].

On the other hand, amorphous and crystalline phases can be assumed to behave as two viscoelastic elements connected in series and carrying the same stress. These assumptions lead to the following relation:

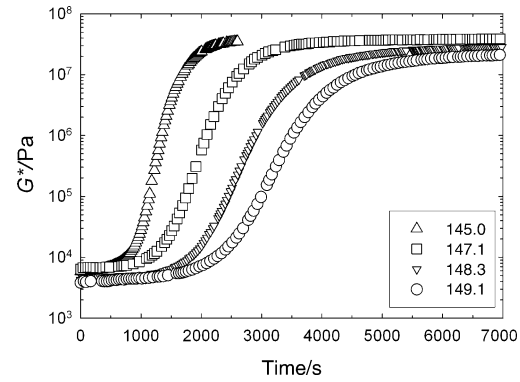

Fig. 8 Time evolution of the complex modulus at an oscillatory frequency of 1 rad s^{-1} during isothermal crystallization in the temperature range between 144.3 and 149.1 °C

$$x(t) = \frac{G^*(t) - G_0^*}{G_\infty^* - G_0^*}\left[\frac{G_\infty^*}{G^*(t)}\right] \quad (5)$$

The crystalline phase can be viewed as rigid filler dispersed in an amorphous (matrix) phase. The two models, described by Eqs 4 and 5 represent, respectively, a lower and an upper limits in the reinforcement due to the presence of the filler.

Much effort has been dedicated to the development of models able to describe the mechanical behaviour of particulate composite systems as a function of filler volume fraction. Nonetheless, a theoretical approach that is able to describe the reinforcement due the crystalline phase is still missing. An empirical power law expression that has already been used [8] to correlate dynamic mechanical measurements to the evolution of crystalline content during isothermal polymer crystallization is the following:

$$x(t) = \frac{G^*(t) - G_0^*}{G_\infty^* - G_0^*}\left[\frac{G_\infty^*}{G^*(t)}\right]^p \quad (6)$$

where p is an empirical power law exponent varying from 0 to 1. It is noticeable that for $p = 1$ Eq. 6 is equivalent to the in-series model and that for $p = 0$ Eq. 6 is equivalent to the in-parallel model.

As the elastic modulus of a crystallizing system is expected to depend upon morphological details of the crystalline phase, Eq. 6 is expected to describe experimental data better than Eqs. 4 and 5.

In Fig. 9 experimental results and predictions of Eq. 6 are compared. A value of $p = 0.89$, independent of temperature, has been obtained by nonlinear fitting procedure.

The good quantitative agreement between experimental data and predictions of Eq. 6 is apparent. The agreement is also confirmed by heat flux data (see insert in Fig. 9). Furthermore, when rheological data treated using Eq. 6 are analysed using Avrami Equation (Eq. 4), the corresponding half-crystallization time and Avrami exponent are in line with those obtained from DSC data as demonstrated by data plotted in Fig. 7.

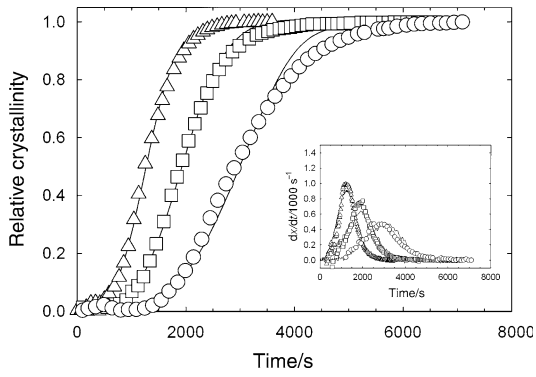

Fig. 9 Time evolution of the relative crystallinity as calculated from DSC data (*solid lines*) and rheological data (*symbols*) treated using Eq. 6. The inset shows the analogous comparison for crystallization rate data

Concluding remarks and perspectives

In this article, we have shown that comparison of calorimetric and rheological results collected during isothermal crystallization of a PP–EPR copolymer is possible after a careful calibration of temperature sensors of the two instruments.

Furthermore, as the complex modulus of a crystallizing system is a monotonically increasing function of relative crystallinity, the evolution of the complex modulus can be related to the evolution of the crystalline fraction. When the modulus increase is converted into relative crystallinity through a power law function, rheological and calorimetric data show an excellent agreement. As a consequence, rheological techniques can be used to complement the study of crystallization kinetics especially at high temperatures, where DSC is not sufficiently sensitive, and to gain more details upon morphological details during solidification.

References

1. Khanna YP. Rheological mechanism and overview of nucleated crystallization. Macromolecules. 1993;26:3639–43.
2. Acierno S, Di Maio E, Iannace S, Grizzuti N. Structure development during crystallization of polycaprolactone. Rheol Acta. 2006;45:387–92.
3. Boutahar K, Carrot C, Guillet J. Crystallization of polyolefins from rheological measurements-relation between the transformed fraction and the dynamic moduli. Macromolecules. 1998;31:1921–9.
4. Kiewiet S, Jassens V, Miltner HE, Van Assche G, Van Puyvelde P, Van Mele B. RheoDSC. A hyphenated technique for simultaneous measurement of calorimetric and rheological evolutions. Rev Sci Instrum. 2008;79:023905 (1–7).
5. Evans UR. The laws of expanding circles and spheres in relation to the lateral growth of surface films and the grain-size of metal. Trans Faraday Soc. 1945;41:365–74.
6. Sajkiewicz P. Transient and athermal effects in the crystallization of polymers. I. Isothermal crystallization. J Polym Sci B Polym Phys. 2002;40:1835–49.
7. Bicerano J. Crystallization of polypropylene and poly(ethylene terephthalate). J Macromol Sci Rev Macromol Chem Phys. 1998;C38:391–479.
8. Kenny JM, Maffezzoli A, Nicolais L. Modeling of the dynamic mechanical properties of semicrystalline thermoplastic matrix composites. Polym Compos. 1992;13:386–93.